

## A Search for Anomalous Heavy-Flavor Quark Production in Association with $W$ Bosons

The DØ Collaboration  
URL <http://www-d0.fnal.gov>  
(Dated: August 11, 2004)

The production of  $W$  bosons in association with jets at the Fermilab Tevatron provides an opportunity to test predictions for electroweak and QCD processes described by the standard model. We present an examination of the exclusive jet spectrum in the  $W$ +jets final state in which the heavy-flavor quark content has been enhanced by requiring at least one  $b$ -tagged jet in an event. We also measure the exclusive jet spectrum for events that contain one jet tagged with more than one algorithm. We compare data on  $e$  + jets ( $164.3 \text{ pb}^{-1}$ ) and  $\mu$  + jets ( $145.3 \text{ pb}^{-1}$ ) channels, collected with the DØ detector during Run II of the Fermilab Tevatron, to expectations from the standard model, and set upper limits on anomalous production of such events.

*Preliminary Results for Summer 2004 Conferences*

## I. INTRODUCTION

The heavy-flavor quark content of jets produced in association with a  $W$  boson provides a sensitive test of standard-model (SM) predictions for such processes. Deviations from expected rates would suggest the presence of physics not described by the SM. The primary contributions to producing a  $W$  boson associated with heavy-flavor quarks in the final state are expected to be from  $t\bar{t}$  and  $Wb\bar{b}$  final states, with additional SM contributions arising from single-top or  $WZ$  (with  $Z \rightarrow b\bar{b}$ ) production.

The production of  $W$  bosons accompanied by light-quarks called  $W + n$ -jet in this note, where the index  $n$  indicates the inclusion of  $n$  or more quark jets) contributes to the background when the light-quark jets are misidentified as heavy-flavor quarks. In addition, background can arise from  $Zb\bar{b}$ ,  $ZZ$  (with one  $Z \rightarrow b\bar{b}$ ), and  $Z + n$ -jet production when one of the leptons from  $Z \rightarrow \ell^+\ell^-$  decay is not observed in the detector. The main instrumental background arises from multijet processes in which a jet is misidentified as a lepton, and missing transverse energy is generated through the mismeasurement of one of the jets. These kinds of events can originate from  $b$ -tagged heavy-flavor jets or misidentified light-quark jets.

Evidence for anomalous production of heavy-flavor (hf) jets in association with a  $W$  boson was reported recently by the CDF collaboration [1]. Our analysis investigates this issue by studying the exclusive jet spectrum using secondary-vertex (SVT) and soft-lepton (SLT)  $b$ -tagging algorithms. To address the anomaly observed by CDF in Run I of the Fermilab Tevatron [1], the exclusive jet spectrum is examined in a richer sample of hf events that contain at least one jet  $b$ -tagged with both SVT and SLT algorithms. The data correspond to  $164.3 \text{ pb}^{-1}$  in the  $e + \text{jets}$  channel and  $145.3 \text{ pb}^{-1}$  in the  $\mu + \text{jets}$  channel, collected with the DØ detector [2] during Run II of the Fermilab Tevatron. We discuss the trigger, methods used for reconstruction and identification of physical objects, event selection, and backgrounds to the  $W + \text{jets}$  final states.

## II. DATA AND BACKGROUNDS

The data for the studies outlined in this note were collected with the DØ detector during Run II of the Fermilab Tevatron. The DØ detector is comprised of the following main elements. A magnetic central-tracking system, which consists of a silicon microstrip tracker (SMT) and a central fiber tracker (CFT), both located within a 2 T superconducting solenoidal magnet [2]. The SMT has  $\approx 800,000$  individual strips, with typical pitch of  $50 - 80 \mu\text{m}$ , and a design optimized for tracking and vertexing capability at pseudorapidities  $|\eta| < 3$ . The system has a six-barrel longitudinal structure, each with a set of four layers arranged axially around the beam pipe, and interspersed with 16 radial disks. The CFT has eight thin coaxial barrels, each supporting two doublets of overlapping scintillating fibers of 0.835 mm diameter, one doublet being parallel to the collision axis, and the other alternating by  $\pm 3^\circ$  relative to the axis. Light signals are transferred via clear light fibers to solid-state photon counters (VLPC) that have  $\approx 80\%$  quantum efficiency.

Central and forward preshower detectors located just outside of the superconducting coil (in front of the calorimetry) are constructed of several layers of extruded triangular scintillator strips that are read out using wavelength-shifting fibers and VLPCs. The next layer of detection involves three liquid-argon/uranium calorimeters: a central section (CC) covering  $|\eta|$  up to  $\approx 1$ , and two end calorimeters (EC) extending coverage to  $|\eta| \approx 4$ , all housed in separate cryostats [3]. In addition to the preshower detectors, scintillators between the CC and EC cryostats provide sampling of developing showers at  $1.1 < |\eta| < 1.4$ .

A muon system resides beyond the calorimetry, and consists of a layer of tracking detectors and scintillation trigger counters before 1.8 T toroids, followed by two more similar layers after the toroids. Tracking at  $|\eta| < 1$  relies on 10 cm wide drift tubes [3], while 1 cm mini-drift tubes are used at  $1 < |\eta| < 2$ . Coverage for muons is partially compromised in the region of  $|\eta| < 1$  and  $|\phi| < 0.2 \text{ rad}$ , where the calorimeter is supported mechanically from the ground [4].

Luminosity is measured using plastic scintillator arrays located in front of the EC cryostats, covering  $2.7 < |\eta| < 4.4$ . A forward-proton detector, situated in the Tevatron tunnel on either side of the interaction region, consists of a total of 18 Roman pots used for measuring high-momentum charged-particle trajectories close to the incident beam directions.

The trigger and data acquisition systems are designed to accommodate the high luminosities of Run II. Based on preliminary information from tracking, calorimetry, and muon systems, the output of the first level of the trigger is used to limit the rate for accepted events to  $\approx 1.5 \text{ kHz}$ . At the next trigger stage, with more refined information, the rate is reduced further to  $\approx 800 \text{ Hz}$ . These first two levels of triggering rely mainly on hardware and firmware. The third and final level of the trigger, with access to all the event information, uses software algorithms and a computing farm, and reduces the output rate to  $\approx 50 \text{ Hz}$ , which is written to tape.

We reject events from data-collection periods in which major subdetectors are not fully functional. In addition, events in which the calorimeter exhibits excessive noise are also rejected. Standard quality criteria are used to identify well-reconstructed electrons, muons, and jets. Energies of electrons and jets are corrected for scale, and jets are

corrected for muon decays within them. The missing transverse energy ( $\cancel{E}_T$ ) contains all energy corrections, including those for any muon in the event. In the selection of  $W \rightarrow e\nu$  and  $W \rightarrow \mu\nu$  decays, we require a single-electron or a single-muon trigger to have fired for each event. The full data sample is reduced to two smaller sub-samples, referred to in the following as the 1EMloose and 1MUloose samples, which are selected as follows:

- **1EMloose:** One reconstructed electromagnetic shower with  $p_T^e > 15$  GeV/c.
- **1MUloose:** One reconstructed muon with  $p_T^\mu > 8$  GeV/c.

The integrated luminosity is  $164.3 \text{ pb}^{-1}$  for the 1EMloose sample and  $145.3 \text{ pb}^{-1}$  for the 1MUloose sample. The uncertainty on the measured value of the luminosity is 6.5% [5].

The single-electron triggers used for this analysis have a minimum Level 1 (L1) trigger requirement of one L1 calorimeter trigger tower with at least 11 GeV of energy in the electromagnetic portion of the calorimeter. Level 3 of the trigger requires a single electron candidate above 20 GeV, with a shower shape requirement on the reconstructed electron candidate. The single-electron triggers are, on average,  $97.0 \pm 1.6\%$  efficient [6]. The single-muon triggers have a L1 trigger requirement of a scintillator trigger in coincidence with a trigger from the luminosity detector (to reject cosmic ray muons). At Level 2, the trigger requires a reconstructed muon with  $p_T > 5$  GeV/c, and at Level 3, one charged track with  $p_T > 10$  GeV/c. The single-muon triggers have an average efficiency of  $59.7 \pm 5.2\%$  [7].

All events with reconstructed primary vertexes (PV) containing less than 3 tracks, or  $z$ -positions (along the beam) of  $|z_{PV}| > 60$  cm from the geometrical center of the detector, are rejected. Candidate events for  $W \rightarrow e\nu$  decays are selected by requiring one isolated, track-matched electron with  $p_T^e > 20$  GeV/c and  $|\eta_e| < 1.1$ . Candidate events for  $W \rightarrow \mu\nu$  decays are selected by requiring one isolated, track-matched muon with  $p_T^\mu > 20$  GeV/c and  $|\eta_\mu| < 1.6$ . A lepton is considered isolated if it has separation of  $\Delta R > 0.5$  in  $(\eta, \phi)$  from all jets in the event. Muons are required to satisfy two additional isolation criteria. First, we require that the transverse energy deposited in the calorimeter in an annular ring (or muon halo), defined by  $0.1 < \Delta R < 0.4$  around the axis of the muon, be smaller than 2.5 GeV. Second, we require that the sum of the  $p_T$  of all tracks in a cone of  $\Delta R < 0.5$  around the muon direction be less than 2.5 GeV/c. Events are also required to have  $\cancel{E}_T > 20$  GeV, and  $\Delta\phi(\ell, \cancel{E}_T) > \pi/8$ . Finally, we select events with a reconstructed transverse mass corresponding to that of the  $W$  boson  $40 < M_{W_T} < 120$  GeV, to enhance  $W$ -boson purity in the sample and to reject background from multijet production. (In calculating  $M_{W_T}$ , we assume that  $\cancel{E}_T$  corresponds to the  $E_T$  of the neutrino).

Upon selection of candidate  $W \rightarrow e\nu$  and  $W \rightarrow \mu\nu$  events, we evaluate the heavy-flavor jet content of the event. We consider only jets with  $p_T^j > 25$  GeV/c and  $|\eta_j| < 2.5$ . Jets that have axes within  $\Delta R < 0.45$  of an electron are rejected to eliminate the ambiguity of electrons also being reconstructed as jets. All jets not satisfying these criteria are removed from the analysis. Jets are then evaluated using the SLT and SVT  $b$ -tagging algorithms.

The SLT algorithm is based on soft muons from decays of heavy-flavor quarks through virtual  $W$  bosons, and relies on muons that are produced near a jet in  $(\eta, \phi)$  space. Only muons with  $p_T^\mu > 4.0$  GeV/c and  $|\eta_\mu| < 2.0$  are considered for  $b$ -tagging. To reject  $Z \rightarrow \mu\mu$  backgrounds, we require  $p_T^\mu < 15.0$  GeV/c. Jets with muons within  $\Delta R < 0.5$  to the jet axis are deemed  $b$ -tagged. In case of ambiguity, the muon closest to the jet axis is chosen as the tagging muon.

Secondary-vertex tags (SVT) are used to identify displaced decay vertices of particles such as B mesons. We use secondary-vertex reconstruction based on a Kalman Filter algorithm [14], which is described in Ref. [15]. To form secondary vertices, charged tracks are selected on the basis of the significance of their distance of closest approach ( $dca$ ) to the PV, or  $dca/\sigma_{dca}$ , where  $\sigma_{dca}$  is the uncertainty on  $dca$ . The transverse decay length of the secondary vertex,  $L_{xy}$ , is taken as the transverse distance from the PV to the beam direction, and is required to be  $< 2.6$  cm. The decay-length significance,  $\frac{L_{xy}}{\sigma_{L_{xy}}}$ , where  $\sigma_{L_{xy}}$  is the estimated uncertainty on  $L_{xy}$ , is required to be  $> 7$ . Jets are considered tagged by this algorithm when a secondary vertex lies within  $\Delta R < 0.5$  of the jet axis. In case of ambiguity, the secondary vertex with the largest number of tracks that overlap the tracks in the entire jet is chosen as the candidate secondary vertex.

To study the predicted SM rates, MC events were generated for the processes mentioned in the Introduction, with the exception of multijet production, which is estimated from data using the selections described below. A summary of the MC processes used in this analysis is given in Table I. The MC events were generated at  $\sqrt{s} = 1.96$  TeV, using the CTEQ5L [12] parton distribution functions (PDFs). A Poisson-distributed minimum-bias overlay, with an average of 0.8 events, was included for all events. The  $t\bar{t}$  MC events were generated with  $m_{top} = 175.0$  GeV.

To avoid incorrect combining of cross sections, the number of jets reconstructed in each event is required to equal the number of initial partons requested for each simulated sample. The  $W/Z + n$ -jets PYTHIA [11] MC is used to normalize the selection before  $b$ -tagging.

The contribution from the process  $Wb$  is estimated from a parametrized MCFM MC [8], and used to calculate a cross section relative to  $Wb\bar{b}$  production. This ratio is  $R_{W+b/W+b\bar{b}} = 0.21$  for events in which all jets are required to have  $p_T > 15$  GeV/c. The cross section for  $Wb$  is taken as this ratio multiplied by the  $Wb\bar{b}$  cross section, which is

MC Type	Generator	$\sigma \times B(pb)$
$t\bar{t} \rightarrow \ell\nu b q\bar{q}\bar{b}$	ALPGEN [9]	2.36
$t\bar{t} \rightarrow \ell\nu b \ell\nu\bar{b}$	ALPGEN	0.59
$t\bar{t} \rightarrow q\bar{q}b q\bar{q}\bar{b}$	ALPGEN	2.36
$tb$ (s-channel), ( $W \rightarrow e, \mu\nu$ )	COMPHEP [10]	0.23
$qtb$ (Wg-fusion), ( $W \rightarrow e, \mu\nu$ )	COMPHEP	0.52
$W(\rightarrow e, \mu\nu)b\bar{b} + jets$	ALPGEN	11.23
$Z(\rightarrow ee, \mu\mu)b\bar{b} + jets$	ALPGEN	1.74
$Z(\rightarrow ee, \mu\mu)b$ ( $Z \rightarrow ee, \mu\mu$ )	PYTHIA [11]	1.54
$W(\rightarrow e, \mu\nu)c\bar{c} + jets$	ALPGEN	11.7
$Z(\rightarrow ee, \mu\mu)c\bar{c} + jets$	ALPGEN	4.63
$W(\rightarrow e, \mu\nu)c + jets$	ALPGEN	125
$W(\rightarrow e, \mu\nu) + n$ -jet ( $n \geq 1$ )	ALPGEN	2575
$Z(\rightarrow ee, \mu\mu) + n$ -jet ( $n \geq 1$ )	ALPGEN	260
$WZ \rightarrow \ell\nu q\bar{q}, q\bar{q}\ell\ell$	ALPGEN	0.72
$ZZ \rightarrow \ell\ell q\bar{q}$	ALPGEN	0.21
$WW \rightarrow \ell\nu q\bar{q}$	ALPGEN	1.20
$W(\rightarrow \ell\nu) + n$ -jet ( $n \geq 0$ )	PYTHIA	9162
$Z(\rightarrow \ell\ell) + n$ -jet ( $n \geq 0$ )	PYTHIA	882

TABLE I: Simulated SM processes contributing to  $e + jets$  and  $\mu + jets$  final states. The cross sections are multiplied by the branching fractions indicated for each process, and represent the total cross section before acceptances. ( $\ell$  refers to all three leptons:  $e, \mu,$  and  $\tau.$ )

normalized to the calculation at next-to-leading order (NLO) [8]. In addition, the  $p_T$  spectrum for  $Wb$  is obtained from PYTHIA inclusive  $W$  production. The expected efficiency for  $Wb$  is then calculated using the efficiency for  $Wb\bar{b}$  events, in which only one jet is reconstructed, convoluted with the efficiency for the jet requirements for the  $Wb$   $p_T$  spectrum.

As mentioned before, the number of multijet events that pass our selections is estimated using data. The background contribution is calculated separately for the  $W \rightarrow e\nu$  and for the  $W \rightarrow \mu\nu$  selections. To determine the expected number of multijet events in any sample, we first define “loose” and “tight” samples that differ through a specific lepton-selection parameter, chosen to admit a significant amount of background into the analysis. For the  $e + jets$  measurement, the loose and tight samples differ by a requirement on an extrapolation of the electron track to match energy deposited in the calorimeter. For the  $\mu + jets$  measurement, the loose and tight samples differ by a requirement on muon halo and on track isolation. The number of multijet “QCD” events for each bin of each distribution can be calculated from the loose and tight samples as follows [13]:

$$N_{QCD} = \epsilon_{fake} \frac{\epsilon_{sig} N_{loose} - N_{tight}}{\epsilon_{sig} - \epsilon_{fake}} \quad (1)$$

where  $N_{loose}$  and  $N_{tight}$  are the number of events selected by the loose and tight selections, respectively,  $\epsilon_{fake}$  is the efficiency for multijet events to mimic the tight event requirement, and  $\epsilon_{sig}$  is the efficiency for  $W$  events to pass the tight event requirement. In this way, the multijet background is estimated for every differential distribution, and is included in the analysis as a separate background contribution. The values of  $\epsilon_{sig}$  are measured in  $Z \rightarrow \ell\ell$  events, where at least one lepton satisfies the tight lepton selection. For events in which the reconstructed  $Z$ -boson mass falls within  $71.2 \text{ GeV} < M_Z < 111.2 \text{ GeV}$ ,  $\epsilon_{sig}$  is measured as the efficiency for the second lepton to pass the tight lepton selection. For estimating  $\epsilon_{fake}$ , we evaluate the number of events that pass full  $W$  selections, except for  $\cancel{E}_T$ , and count the number of events that pass the loose and tight selections in the kinematic region of  $\cancel{E}_T < 20 \text{ GeV}$ . This region is dominated by multijet events, with essentially no  $W$  bosons present, and therefore provides a good estimate of the rate for misidentification of jets.

### III. RESULTS OF ANALYSIS

Figure 1 shows the distributions in transverse momentum of electron candidates and of  $\cancel{E}_T$  for data and MC in the  $W \rightarrow e\nu$  selection. Also included in the figures is the estimated multijet background. Figure 2 shows the distribution in the transverse mass of the  $W$ , and the  $p_T$  of the  $W$ , derived from the transverse momentum of the electron and  $\cancel{E}_T$ .

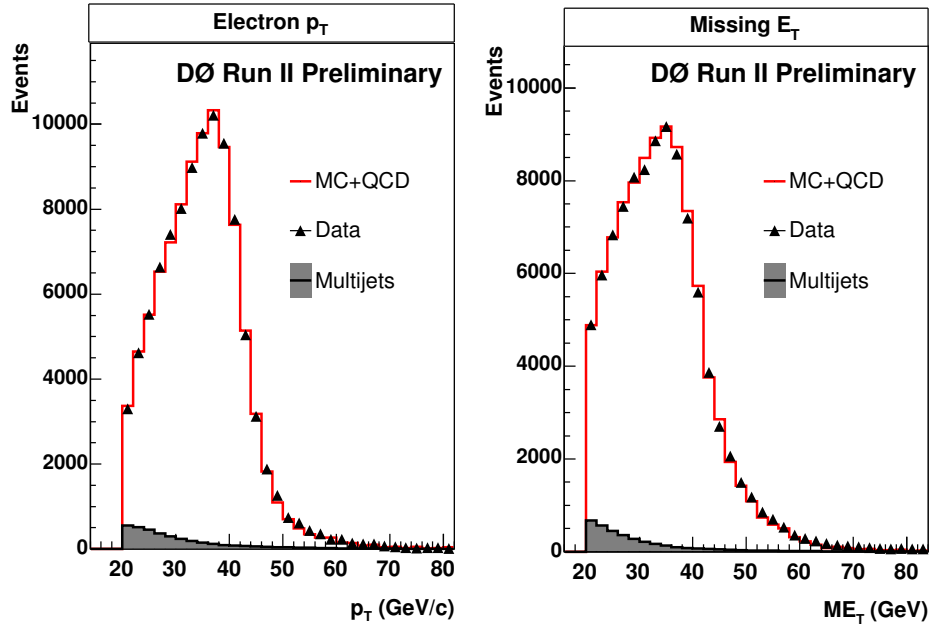


FIG. 1: Electron  $p_T$  and missing transverse energy in the  $W \rightarrow e\nu$  channel, prior to requiring  $b$ -tagging. The MC is based on the PYTHIA generator.

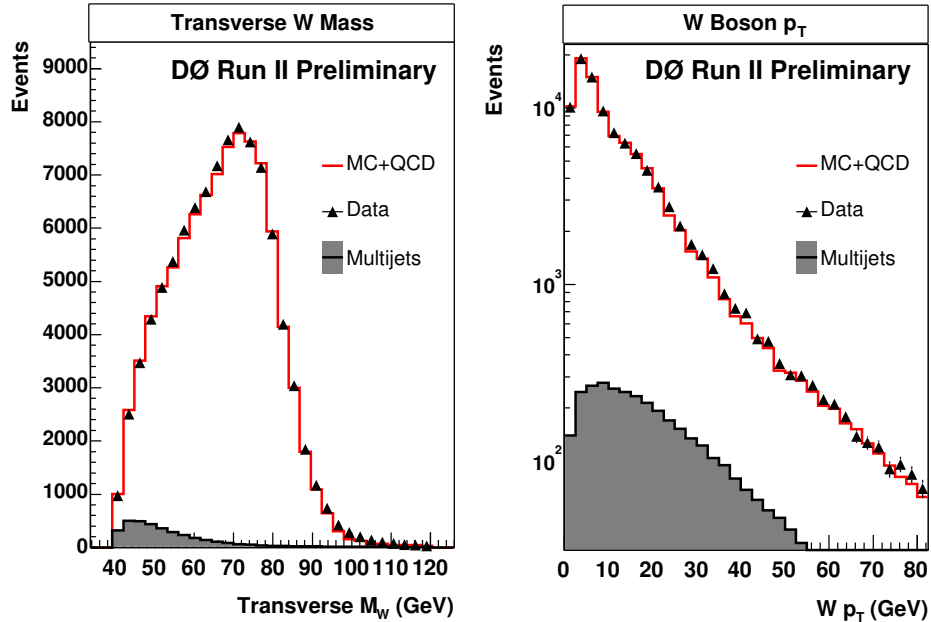


FIG. 2: Transverse mass of  $W$  bosons, and their  $p_T$  in the  $W \rightarrow e\nu$  channel, prior to requiring  $b$ -tagging. The MC is based on the PYTHIA generator.

In Figs. 3 and 4, we show the analogous distributions for  $W \rightarrow \mu\nu$ . All four distributions do not involve  $b$ -tagging, and represent a normalization of the inclusive PYTHIA  $W/Z + n$ -jet MC to data. The observed shapes are in adequate agreement with the MC expectation.

Figure 5 shows the exclusive number of jets in events with a selected  $W$  boson. The fourth bin in the plot includes the sum of four or more jets. The number of expected and observed events for this distribution is shown in table II.

After selecting  $W$ -boson candidates, and restricting the reconstructed transverse mass to the peak of the  $W$ , we apply the two selected  $b$ -tagging algorithms to the events. When an event has at least one tagged jet, it is kept for

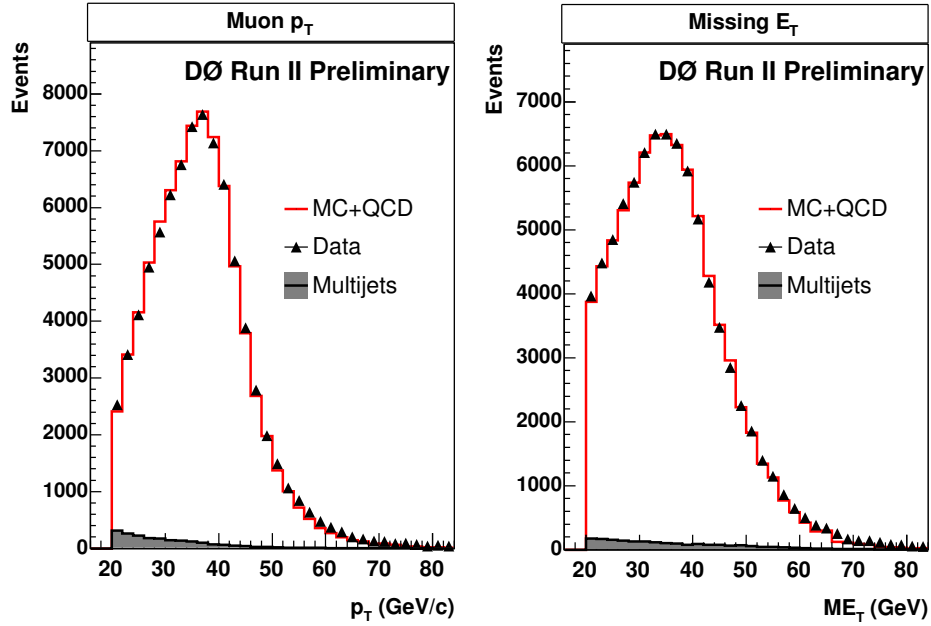


FIG. 3: Muon  $p_T$  and missing transverse energy in the  $W \rightarrow \mu\nu$  channel, prior to requiring  $b$ -tagging. The MC is based on the PYTHIA generator.

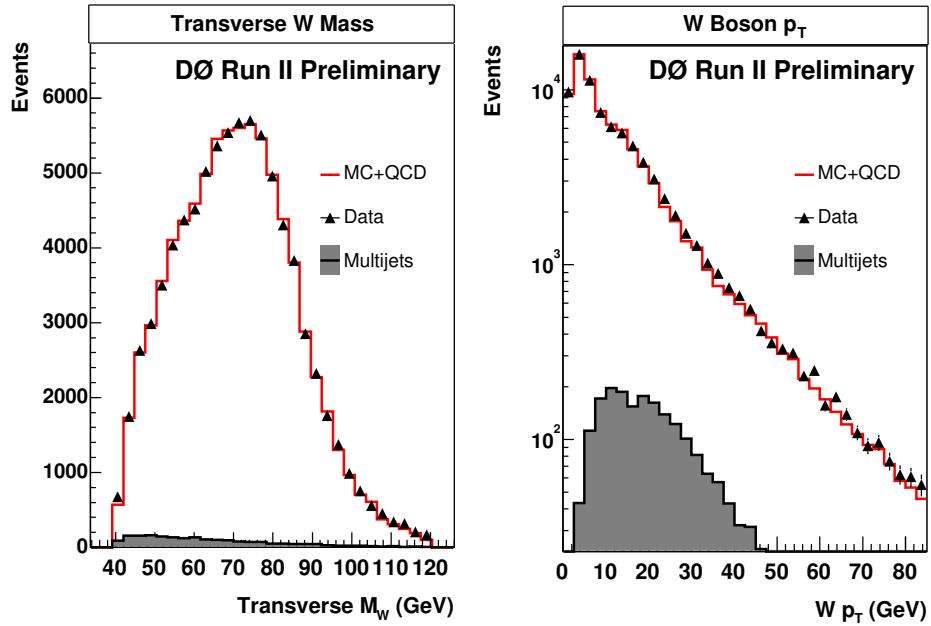


FIG. 4: Transverse mass of  $W$  bosons, and their  $p_T$  in the  $W \rightarrow \mu\nu$  channel, prior to requiring  $b$ -tagging. The MC is based on the PYTHIA generator.

the next stage of analysis. For each algorithm, we handle separately the distribution of events for the  $e$ +jets and  $\mu$ +jets selections, because the samples have different integrated luminosities. After a renormalization, we sum the two samples to improve the statistical uncertainty of the analysis. The MC is corrected for differences relative to data in  $b$ -tagging efficiencies and lepton ID efficiencies. Also, any discrepancy in trigger efficiency between MC and data is corrected for each set of selections ( $e$  + jets and  $\mu$  + jets) [16].

Figure 6 shows the exclusive number of jets in events with at least one SVT-tagged jet. The last bin in the plots contains the sum of four or more jets (there can be more than one SVT-tagged jet in any event.) The distribution of

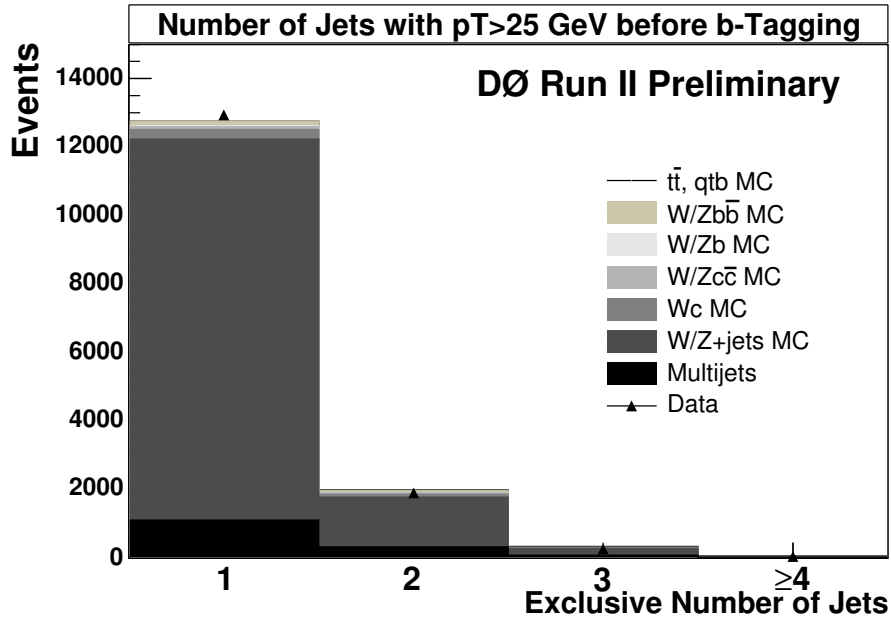


FIG. 5: The exclusive number of jets with  $p_T > 25$  GeV/c in events with a selected  $W$  boson, prior to requiring  $b$ -tagging.

Source	$W+1\text{jet}$	$W+2\text{jets}$	$W+3\text{jets}$	$W+\geq 4\text{jets}$
$W/Z+\text{jet}$	$11146\pm 2190$	$1448\pm 284$	$203\pm 40$	$25\pm 5$
Multijet	$1113\pm 391$	$323\pm 114$	$80\pm 28$	$23\pm 8$
$WW, WZ, ZZ$	$11.2\pm 1.8$	$14.9\pm 2.4$	$1.2\pm 0.2$	$0.1\pm 0.01$
$Wc$	$274.9\pm 54.0$	$83.8\pm 16.5$	$13.6\pm 2.7$	$1.6\pm 0.3$
$W/Zc\bar{c}$	$97.5\pm 19.2$	$37.7\pm 7.4$	$6.2\pm 1.2$	$0.5\pm 0.1$
$W/Zb$	$20.7\pm 4.1$	$7.8\pm 1.5$	$1.2\pm 0.2$	$0.1\pm 0.02$
$W/Zb\bar{b}$	$127.1\pm 25.0$	$60.9\pm 12.0$	$11.1\pm 2.2$	$0.9\pm 0.2$
$t\bar{t}$ , Single top	$6.6\pm 1.0$	$21.2\pm 3.4$	$21.8\pm 3.4$	$15.5\pm 2.5$
SM prediction	$12796\pm 2685$	$1997\pm 441$	$338\pm 78$	$66\pm 16$
Data	12928	1899	289	58

TABLE II: Summary of the exclusive number of jets with  $p_T > 25$  GeV/c in events with a selected  $W$  boson, prior to requiring  $b$ -tagging.

expected and observed events with at least one SVT  $b$ -tagged jet is summarized in Table III.

Figure 7 shows the exclusive number of jets in events with at least one SLT-tagged jet. The format for these plots is the same as that for the SVT plots in the previous paragraph. The distribution of expected and observed events with at least one SLT  $b$ -tagged jet is summarized by source in Table IV.

Jets tagged with both algorithms should provide a cleaner sample of heavy-flavor jets. The results for such events with at least one “doubly-tagged” jet, supposedly enriched in heavy-quark content is shown in Fig. 8. The distribution of expected and observed events with at least one jet tagged by both the SLT and SVT algorithms is summarized in Table V.

Figure 9 shows the distribution of the measured transverse  $W$ -boson mass for events in which at least one jet was  $b$ -tagged with either the SVT or SLT tagging algorithms. Here we see no significant departure from the transverse mass distributions obtained before  $b$ -tagging.

The dominant sources of experimental uncertainty in this analysis are listed in Table VI. The largest sources are common to both the  $e + \text{jets}$  and  $\mu + \text{jets}$  selections:

- A 6.5% uncertainty on the integrated luminosity
- Uncertainties arising from the jet-energy scale (JES) corrections and jet identification
- Uncertainties arising from the  $b$ -tagging algorithms

Source	W+1jet	W+2jets	W+3jets	W+ $\geq$ 4jets
W/Z+jet	56.1 $\pm$ 11.0	7.2 $\pm$ 1.4	3.8 $\pm$ 0.7	0.6 $\pm$ 0.1
Multijet	13.4 $\pm$ 4.7	6.8 $\pm$ 2.4	1.5 $\pm$ 0.5	0.6 $\pm$ 0.2
WW,WZ,ZZ	0.26 $\pm$ 0.04	0.71 $\pm$ 0.11	0.08 $\pm$ 0.01	0.01 $\pm$ 0.01
Wc	10.7 $\pm$ 2.1	3.8 $\pm$ 0.8	0.8 $\pm$ 0.2	0.1 $\pm$ 0.02
W/Zc $\bar{c}$	2.2 $\pm$ 0.4	1.8 $\pm$ 0.4	0.41 $\pm$ 0.08	0.05 $\pm$ 0.01
W/Zb	2.8 $\pm$ 0.6	1.8 $\pm$ 0.4	0.32 $\pm$ 0.06	0.03 $\pm$ 0.01
W/Zb $\bar{b}$	13.9 $\pm$ 2.7	12.4 $\pm$ 2.4	2.7 $\pm$ 0.5	0.23 $\pm$ 0.04
t $\bar{t}$ , Single top	1.0 $\pm$ 0.2	5.0 $\pm$ 0.8	6.2 $\pm$ 1.0	5.1 $\pm$ 0.8
SM prediction	100.3 $\pm$ 21.7	39.5 $\pm$ 8.6	15.7 $\pm$ 3.1	6.6 $\pm$ 1.2
Data	104	37	18	6

TABLE III: Summary of observed and predicted  $W$ -boson events with at least one SVT  $b$ -tagged jet.

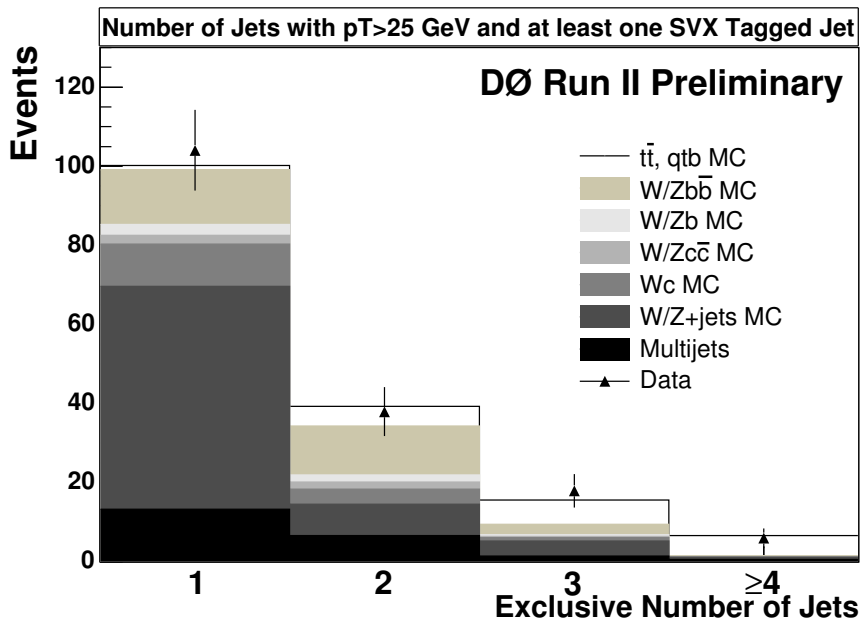


FIG. 6: Exclusive jet multiplicity for events with at least one SVT  $b$ -tagged jet. The fourth bin represents the integral for 4 or more jets.

- Uncertainties associated with modeling trigger efficiencies in MC

The  $e +$  jets selection has additional uncertainties from the identification and reconstruction of electrons as well as from the charged-track-matching to EM clusters. Likewise, the  $\mu +$  jets selection has uncertainties specific to muon identification and reconstruction, as well as from the  $p_T$  resolution of muons. We associate a conservative uncertainty of 15% on the cross sections used to normalize the  $W + X$  ALPGEN MC samples (where  $X$  includes all quark flavors). For the remaining MC samples, we use a value of 10%.

Using the doubly-tagged jet sample, we can set a limit on the rate of anomalous heavy-flavor quark production in association with a  $W$  boson. Because we have not suggested a possible model for such event production, we cannot base this limit on any specific efficiency or exclusive jet spectrum. In the absence such a model, we quote limits on the number of expected events per exclusive jet bin. To determine limits, we calculate the 95% confidence level (C.L.) for additional event production in each bin. We find a limit for each bin by first populating a normalized Poisson distribution with a mean value given by the expected sum of the number of any anomalous-signal and SM-background events,  $N_{s+b}$ . We define  $N_{s+b} = N_s + N_b$ , where  $N_s$  is the hypothesized anomalous production and  $N_b$  is the SM expectation. Next, we define the value  $CL_s$  as the integral of the Poisson distribution above the observed number of events in data. We then determine the value of  $N_s$  for which  $CL_s$  exceeds 0.95. This  $N_s$  is defined as the 95% C.L. limit for the event rate for anomalous heavy-flavor production in association with a  $W$  boson. Table VII shows the values extracted for each jet bin.

Source	$W+1\text{jet}$	$W+2\text{jets}$	$W+3\text{jets}$	$W+\geq 4\text{jets}$
$W/Z+\text{jet}$	$49.9\pm 9.8$	$10.0\pm 2.0$	$3.0\pm 0.6$	$0.24\pm 0.05$
Multijet	$10.2\pm 3.6$	$3.9\pm 1.4$	$1.2\pm 0.4$	$0.51\pm 0.18$
$WW, WZ, ZZ$	$0.15\pm 0.02$	$0.34\pm 0.05$	$0.04\pm 0.01$	$0.01\pm 0.01$
$Wc$	$8.3\pm 1.6$	$2.0\pm 0.4$	$0.65\pm 0.13$	$0.05\pm 0.01$
$W/Zc\bar{c}$	$2.0\pm 0.4$	$1.42\pm 0.28$	$0.30\pm 0.06$	$0.02\pm 0.003$
$W/Zb$	$1.2\pm 0.2$	$0.80\pm 0.16$	$0.13\pm 0.03$	$0.02\pm 0.003$
$W/Zb\bar{b}$	$5.6\pm 1.1$	$5.1\pm 1.0$	$1.1\pm 0.2$	$0.12\pm 0.02$
$t\bar{t}, \text{Single top}$	$0.34\pm 0.05$	$1.7\pm 0.3$	$2.1\pm 0.3$	$1.8\pm 0.3$
SM prediction	$77.7\pm 16.9$	$25.3\pm 5.5$	$8.5\pm 1.8$	$2.8\pm 0.6$
Data	81	21	8	2

TABLE IV: Summary of observed and predicted  $W$ -boson events with at least one SLT  $b$ -tagged jet.

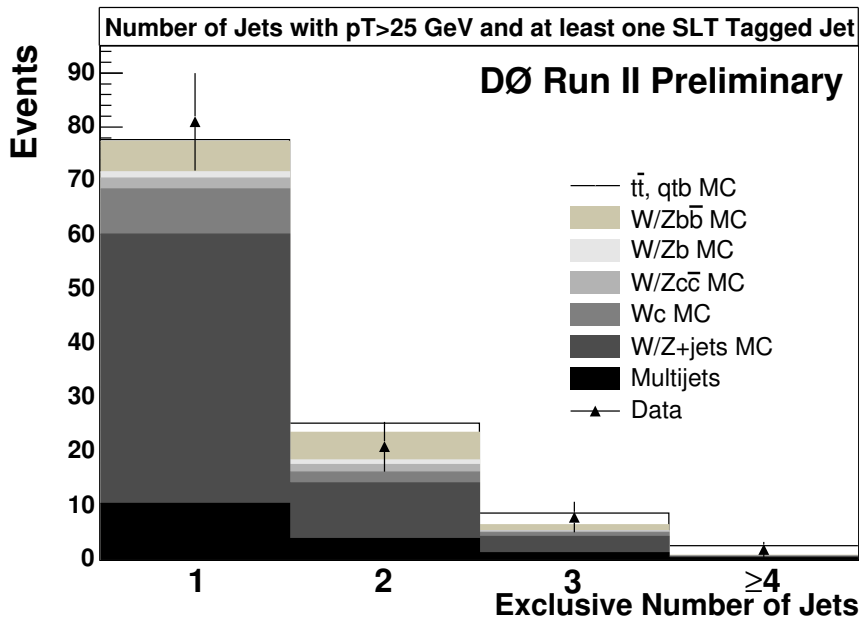


FIG. 7: Exclusive jet multiplicity for events with at least one SLT  $b$ -tagged jet. The fourth bin represents the integral for 4 or more jets.

Assuming that anomalous heavy-flavor production has the same event topology as some SM process, the limits derived above can be translated into limits on cross sections. To this end, we consider two scenarios:

- “ $Wb\bar{b}$ -like” production in which two  $b$  quarks are produced in association with a  $W$  boson. In this scenario, additional light quarks can be included, thereby shifting the event topology to more than 2 jets. Jets not falling within the acceptances of the detector can also cause the event topology to drop to less than 2 jets. We model this production using the efficiencies expected for SM  $W/Z + b\bar{b}$  ALPGEN MC.
- “top-like” production in which a heavy particle is produced and subsequently decays to a  $W$  boson and a  $b$  quark. The event can contain two such heavy particles (“ $t\bar{t}$ -like”) or one heavy quark (“single-top-like”), with additional light or heavy quarks possible for both cases. We model this scenario using the efficiencies expected for SM  $t\bar{t}$  and single-top production.

We evaluate a limit on exclusive jet production for each scenario, but first ignore the efficiency for reconstructing the predicted jets. The remaining efficiency represents  $W$ -boson selection and  $b$ -tagging. To extract limits for a specific model, this efficiency must be multiplied by the efficiency to reconstruct the number of jets given in each exclusive jet bin. These results are shown in Table VIII.

To evaluate a limit on inclusive jet production for each scenario, we reintroduce the efficiency for reconstructing the predicted jets. For inclusive  $Wb\bar{b}$ -like anomalous production, we sum the first two exclusive  $W + n$ -jet bins, as

Source	$W+1\text{jet}$	$W+2\text{jets}$	$W+3\text{jets}$	$W+\geq 4\text{jets}$
$W/Z+\text{jet}$	$2.0\pm 0.4$	$0.05\pm 0.01$	$0.14\pm 0.03$	$0.0\pm 0.0$
Multijet	$1.2\pm 0.4$	$0.5\pm 0.2$	$0.1\pm 0.1$	$0.0\pm 0.0$
$W/Zb, W/Zc$	$0.57\pm 0.11$	$0.13\pm 0.03$	$0.04\pm 0.01$	$0.01\pm 0.003$
$W/Zb\bar{b}, W/Zc\bar{c}$	$0.87\pm 0.17$	$0.84\pm 0.16$	$0.19\pm 0.04$	$0.02\pm 0.004$
$t\bar{t}$ , Single Top	$0.07\pm 0.01$	$0.31\pm 0.05$	$0.43\pm 0.07$	$0.32\pm 0.05$
SM prediction	$4.8\pm 1.1$	$1.9\pm 0.4$	$0.9\pm 0.2$	$0.3\pm 0.1$
Data	5	1	1	0

TABLE V: Summary of observed and predicted  $W$ -boson events with at least one jet tagged by both the SLT and SVT algorithms.

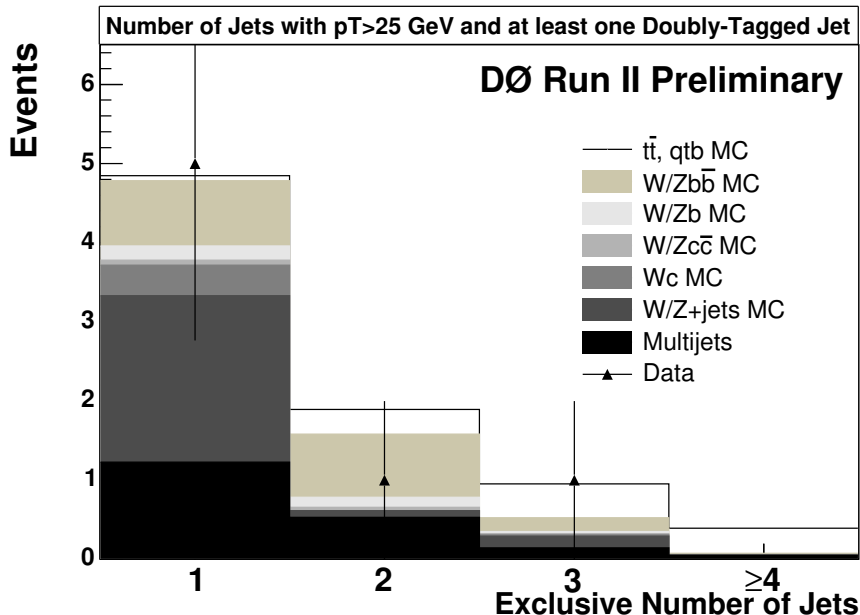


FIG. 8: Exclusive jet multiplicity of events with at least one jet that has been tagged with both the SVT and SLT algorithms. The fourth bin represents the integral for 4 or more jets.

the contribution from the remaining bins is negligible. For  $t\bar{t}$ -like anomalous production, we sum all  $W+n$ -jet bins, except for the  $n=1$  bin where, the contribution is also negligible. Table IX shows the 95% C.L. event limits for the combination of jet bins for these two hypotheses, and also the corresponding anomalous heavy-flavor production cross-section limit. The jet reconstruction efficiency is included in the calculations, and the limits contain the expected efficiency for the specified SM processes.

#### IV. CONCLUSIONS

We have presented an analysis of events in which a  $W$  boson was selected in either the  $W \rightarrow e\nu$  or  $W \rightarrow \mu\nu$  decay channel. After this selection, we examined the jets in these events for possible  $b$ -tags, using both secondary-vertex and soft-muon  $b$ -tagging algorithms. In the  $e + \text{jets}$  channel we analyzed  $164.3 \text{ pb}^{-1}$  of data, and  $145.3 \text{ pb}^{-1}$  of data in the  $\mu + \text{jets}$  channel. At this time, we see no significant departure from the predictions of the standard model (see Figs. 6-8), and we set a 95% CL limit on the rate of anomalous production as a function of the number of jets in the events in which at least one jet is  $b$ -tagged with a simultaneous SLT and SVX  $b$ -tagging algorithm (see Table VII). Interpreting these results as anomalous SM production of either  $Wb\bar{b}$ -like events or top-like events, we are able to set cross-section limits of 25.0 pb and 9.3 pb, respectively, for such additional processes (see Table IX).

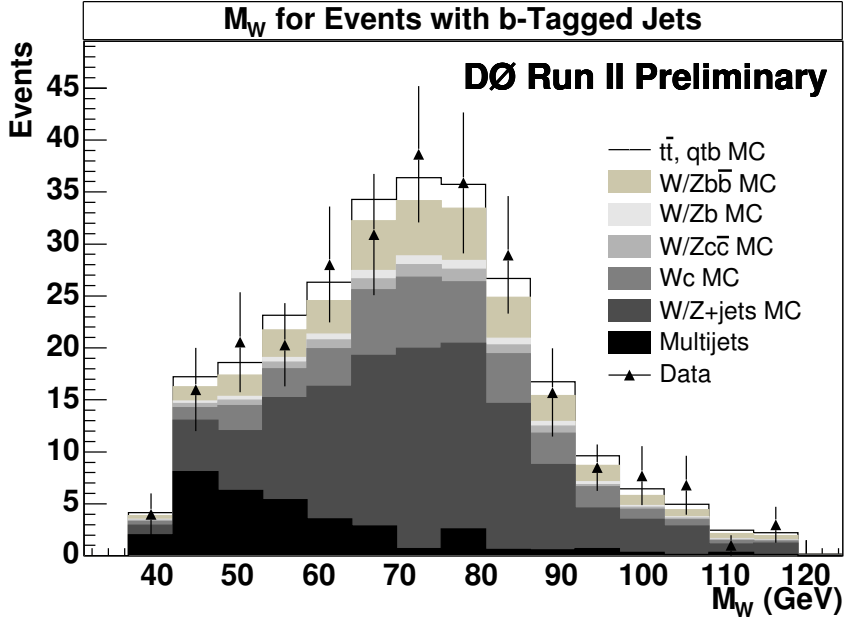


FIG. 9: Transverse  $W$ -boson mass for events with at least one  $b$ -tagged jet.

Systematic	$N_{jet} = 1$	$N_{jet} = 2$	$N_{jet} = 3$	$N_{jet} \geq 4$
$em_{ID}$	$\pm 2.1\%$	$\pm 2.1\%$	$\pm 2.1\%$	$\pm 2.1\%$
$em_{trk}$	$\pm 3.1\%$	$\pm 3.1\%$	$\pm 3.1\%$	$\pm 3.1\%$
$\mu_{ID}$	$\pm 0.8\%$	$\pm 0.8\%$	$\pm 0.8\%$	$\pm 0.8\%$
$\mu_{pT}$	$\pm 3.0\%$	$\pm 3.0\%$	$\pm 3.0\%$	$\pm 3.0\%$
Lumi	$\pm 6.5\%$	$\pm 6.5\%$	$\pm 6.5\%$	$\pm 6.5\%$
Electron Trigger	$\pm 2.0\%$	$\pm 2.0\%$	$\pm 2.0\%$	$\pm 2.0\%$
Muon Trigger	$\pm 5.2\%$	$\pm 5.2\%$	$\pm 5.2\%$	$\pm 5.2\%$
MC Cross Section	$\pm 10 - \pm 15\%$			
JES	$\pm 2.0\%$	$\pm 2.0\%$	$\pm 2.0\%$	$\pm 2.0\%$
Jet ID	$\pm 4.0\%$	$\pm 4.0\%$	$\pm 4.0\%$	$\pm 4.0\%$
SVT $b$ -tagging	$\pm 9.5\%$	$\pm 9.5\%$	$\pm 9.7\%$	$\pm 9.7\%$
SLT $b$ -tagging	$\pm 8\%$	$\pm 8\%$	$\pm 8\%$	$\pm 8\%$
Parton matching	$\pm 3\%$	$\pm 3\%$	$\pm 3\%$	$\pm 3\%$

TABLE VI: Summary of systematic uncertainties associated with results for  $b$ -tagged jets, as a function of the total exclusive number of jets, including any tagged jets.

### Acknowledgments

We thank the staffs at Fermilab and collaborating institutions, and acknowledge support from the Department of Energy and National Science Foundation (USA), Commissariat à L'Énergie Atomique and CNRS/Institut National de Physique Nucléaire et de Physique des Particules (France), Ministry for Science and Technology and Ministry for Atomic Energy (Russia), CAPES, CNPq and FAPERJ (Brazil), Departments of Atomic Energy and Science and Education (India), Colciencias (Colombia), CONACyT (Mexico), Ministry of Education and KOSEF (Korea), CONICET and UBACyT (Argentina), The Foundation for Fundamental Research on Matter (The Netherlands), PPARC (United Kingdom), Ministry of Education (Czech Republic), Natural Sciences and Engineering Research Council and West-Grid Project (Canada), BMBF (Germany), A.P. Sloan Foundation, Civilian Research and Development Foundation,

Source	$W+1\text{jet}$	$W+2\text{jets}$	$W+3\text{jets}$	$W+\geq 4\text{jets}$
Data observation	5	1	1	0
SM prediction	$4.8\pm 1.1$	$1.9\pm 0.4$	$0.9\pm 0.2$	$0.3\pm 0.05$
95% C.L. Limit (events)	6.78	3.88	4.17	3.0

TABLE VII: Observed and predicted  $W$ -boson events with at least one jet tagged by both the SLT and SVT algorithms. Also shown is the 95% C.L. limit in the form of additional expected events.

Model	$W+1\text{jet}$	$W+2\text{jets}$	$W+3\text{jets}$	$W+\geq 4\text{jets}$
Top-like	13.3	8.3	11.7	16.1
$Wb\bar{b}$ -like	36.7	9.6	6.3	4.8

TABLE VIII: Cross-section limits in pb, based on the hypotheses of “top-like” anomalous production and “ $Wb\bar{b}$ -like” anomalous production of exclusive number of jets. Each value is corrected for the efficiency of reconstructing the predicted number of jets in each jet bin.

Research Corporation, Texas Advanced Research Program, and the Alexander von Humboldt Foundation.

- 
- [1] D. Acosta *et al.* “Study of the heavy flavor content of jets produced in association with  $W$  bosons in  $p\bar{p}$  collisions at  $\sqrt{s} = 1.8$  TeV.” Phys. Rev. D **65**, 052007 (2002).
  - [2] V. Abazov, et al., in preparation for submission to Nucl. Instrum. Methods Phys. Res. A, and T. LeCompte and H.T. Diehl, “The CDF and D0 Upgrades for Run II”, Ann. Rev. Nucl. Part. Sci. **50**, 71 (2000).
  - [3] S. Abachi, *et al.*, Nucl. Instrum. Methods Phys. Res. A **338**, 185 (1994).
  - [4] H. T. Diehl, DØ Note 4088, January, 2003
  - [5] The DØ Luminosity ID Group: [http://www-d0.fnal.gov/phys\\_id/luminosity/](http://www-d0.fnal.gov/phys_id/luminosity/)
  - [6] Pending DØ Note by Doug Chapin, Harald Fox, John Gardner, Robert Illingworth, Adam Lyon, and Junjie Zhu, “Measurement of  $Z \rightarrow ee$  and  $W \rightarrow e\nu$  Production Cross Sections with  $|\eta| < 2.3$ ”
  - [7] Pending DØ Note by Andrew Alton, Andrew Askew, Yuri Maravin, and Sean Mattingly, “Measurement of  $W\gamma$  events in DØ Run II Data”
  - [8] MCFM monte carlo simulator: <http://mcfm.fnal.gov/>
  - [9] ALPGEN, a generator for hard multiparton processes in hadronic collisions, M.L. Mangano, M. Moretti, F. Piccinini, R. Pittau, A. Polosa, JHEP 0307:001,2003, hep-ph/0206293.
  - [10] COMPHEP, A.Pukhov, E.Boos, M.Dubinina, V.Edneral, V.Ilyin, D.Kovalenko, A.Kryukov, V.Savrin, S.Shichanin, and A.Semenov. Preprint INP MSU 98-41/542, hep-ph/9908288
  - [11] PYTHIA 6.154: T. Sjstrand, P. Edn, C. Friberg, L. Lnnblad, G. Miu, S. Mrenna and E. Norrbin, Computer Phys. Commun. 135 (2001) 238 (LU TP 00-30, hep-ph/0010017)
  - [12] H. L. Lai *et al.* [CTEQ Collaboration], “Global QCD analysis of parton structure of the nucleon: CTEQ5 parton distributions,” Eur. Phys. J. C **12** (2000) 375 [arXiv:hep-ph/9903282].
  - [13] S. Beauceron, G. Bernardi, and S. Trincaz-Duvoid, DØ Note 4224
  - [14] Vertex Reconstruction by means of the method of Kalman Filtering, Rolf Luchsinger and Christoph Grab. Computer Physics Communications 76 (1993) 263-280.
  - [15] A. Schwartzman and M. Narain,  $b$ -quark Jet Identification via Secondary Vertex Reconstruction, DØ Note 4080.
  - [16] Pending DØ Note by Wade Fisher, “A Search for Anomalous Heavy-Flavor Quark Production in Association with  $W$  Bosons”

Source	$W+1,2\text{jets}$	$W+2,3,4\text{jets}$
Data observation	6	2
SM prediction	$6.7\pm 1.3$	$3.2\pm 0.5$
95% C.L. Limit (events)	6.72	4.45
Model		
Top-like	-	15.6 pb
$Wb\bar{b}$ -like	27.8 pb	-

TABLE IX: 95% C.L. limits for the number of events summed over the indicated jet bins. Also shown are cross-section limits based on the hypotheses of “top-like” anomalous production and “ $Wb\bar{b}$ -like” anomalous production for the selected numbers of jets.